6. Influence of Lithium Chloride on the Morphology of Flexible Slabstock Polyurethane Foams and Their Plaque Counterparts

6.1 Chapter Summary

In continuing efforts to understand urea phase connectivity in flexible polyurethane foams and its implications on physical properties, LiCl is used to alter the phase-separation behavior of slabstock foams. Comparisons are also drawn with plaque counterparts, which are prepared using the same polyol, isocyanate, and chain extender (water). LiCl is shown to alter the solid-state phase separation behavior of the foams and the plaques in a similar manner. This is confirmed using multiple characterization techniques, which provide information at different scale lengths. The foams and plaques with and without LiCl are shown to possess a microphase separated morphology with interdomain spacings of ca. 100 Å. SAXS and TEM reveal that addition of LiCl reduces the urea aggregation behavior, typical in slabstock polyurethane foams, leading to a loss in the urea phase *macro* connectivity. Hard segment ordering, as studied by WAXS and FTIR, is shown to be of a similar nature in the plaque and foam, which do not incorporate LiCl. Addition of LiCl leads to a loss in the segmental packing behavior, or *micro* level connectivity of the urea phase, in both the plaques and corresponding foams, as inferred from WAXS and FTIR. The LiCl additive interacts with the polyol soft segments in an insignificant manner as shown from FTIR and DMA. In addition, foams containing LiCl are found to possess more intact cell windows due to the influence of LiCl on reaction kinetics as well as its effect on the precipitation of the urea phase. The experimental observations are supported by quantum mechanical calculations using a Density-Functional-Theory (DFT) approach, where molecular interactions between LiCl and model ether, urethane, and urea compounds are investigated. Interaction geometries of most stable complexes and their stability energies are calculated. Stability energies of ether/LiCl, urethane/LiCl, and urea/LiCl were determined to be –189, –617, and –687 kJ/mole respectively, reinforcing that LiCl interacts predominantly with urea hard segments and in a minimal manner with the polyol soft segments.

6.2 Introduction

One of the many applications of polyurethanes (PU) [1,2] lies in the area of flexible foams [1,3], which are used in many areas. Their preparation involves simultaneously occurring

isocyanate-water and isocyanate-polyol reactions. The 'blow' reaction, in which water reacts with an isocyanate (functionality = 2), leads to the formation of urea based hard segments (HS). In the 'gelation' reaction, an isocyanate group reacts with a terminal hydroxyl group of a polyol (functionality > 2) to form urethane linkages, which covalently bond the urea hard segments to the polyol soft segments (SS). As these reactions proceed, the morphology of flexible PU foams develops over several scale lengths. The exotherms associated with these reactions as well as the carbon dioxide generated in the 'blow' reaction helps to expand the foaming mixture into a final cellular structure. Cell sizes in flexible PU foams are typically a few hundred microns in dimensions. The morphology development in the struts of the foam takes place at a much smaller scale length as compared to the cellular structure. The presence of a microphase separated morphology in flexible PU foams was first confirmed using small angle x-ray scattering (SAXS) by Wilkes and coworkers [4]. Their work suggested the formation of urea microdomains separated from the polyol phase with an interdomain spacing of ca. 100 Å. Ever since, SAXS has been a widely utilized technique to understand the fine structure of PU foams [3,5,6].

The presence of morphological features at a scale length greater than the microphase separated fine structure was first reported in a systematic study carried out by Armistead et al [7]. On studying a systematic series of foams, the workers observed that as the HS content was increased, aggregation of the urea microdomains led to the formation of urea rich regions referred to as urea balls/aggregates. Recent work by Ade et al [8] and Rightor et al [9] using x-ray microscopy has focused on elucidating the structure and composition of the urea aggregates.

Earlier work from the same laboratory has utilized 'plaques' based on slabstock as well as molded flexible PU foam formulations in order to study their solid-state morphology [10,11]. Since plaques do not possess a cellular structure, this enables deconvolution of the effects of cellular structure and the solid-state phase-separated morphology on physical properties. Certain morphological differences in the urea aggregation behavior have been noted on comparing the plaques (which do not contain a surfactant) with actual foams (which incorporate a surfactant). However, on making comparisons of structure-property relationships of plaques with their foam counterparts, it has been noted that *both classes of materials display similar trends* thus rationalizing the investigation of plaques to *indirectly* study PU foams [7,12]. A comparison of the structure-property relationships of plaques vs. foams will also be made in the present study.

The subject of HS connectivity in linear PU elastomers has been addressed previously [13]. On investigating a series of PU elastomers with HS contents of 15, 25, 35, and 45 wt%, Abouzahr et al proposed the formation of an interconnected HS morphology at relatively higher HS contents (> 25 wt%). They suggested that randomly dispersed microdomains existed in the polyol matrix when the HS content was less than 25 wt%. The authors reasoned, based on volume fraction arguments, that on exceeding this HS content some level of continuity in the hard phase would be inevitable. Seymour and Cooper have also hypothesized that above a certain HS content, ca. 25 %, it would be impossible, due to spatial limitations, to have discrete separated HS domains resulting in the formation of an interlocking HS morphology [14].

Recent work from this laboratory has focused on examining the urea phase connectivity in formulations based on flexible PU foams [10,11,15]. This has been primarily done using lithium salts as additives in the foam formulations, and extends from the work carried out by Moreland et al [16]. These salts disrupt the hydrogen bonding which is present in the polymer and therefore result in an alteration of the morphology. It was observed that addition of LiCl in both slabstock as well as molded foam formulations led to a reduction in the physical associations of the urea aggregates and thus led to a loss in the urea phase *macro* connectivity [10,11]. It was also shown that addition of LiCl disrupted the packing of the urea HS and thus led to a loss in the urea phase *micro* connectivity, or domain cohesiveness [10,11]. The present study will establish that the earlier findings, which were based on plaque materials, can also be extended to actual PU foams (which incorporate a surfactant).

Surfactants utilized in flexible PU foams are polysiloxane-polyoxyalkylene graft copolymers [1,3,17]. Surfactants perform a variety of functions, the most important ones being reducing surface tension, emulsifying incompatible ingredients, and stabilizing the cell walls. The siloxane block lowers the bulk surface tension, whereas the polyoxyalkylene promotes solubilization of the surfactant into the polyol and aids in emulsification of the foaming components. A detailed study of the influence of a commonly utilized commercial surfactant TEGOSTAB® BF2370, on the structure and properties of slabstock PU foams was carried out recently by Kaushiva and coworkers [18]. The workers noted that the presence of a surfactant affected the urea phase aggregation and resulted in smaller aggregates as compared to a similar formulation, which did not include a surfactant. It was also established that collapse of the

cellular structure prior to the urea precipitation altered the aggregation behavior of the urea phase, further suggesting that the surfactant does influence the phase separation.

This study compares the morphologies developed in slabstock PU foams and their plaque counterparts with and without LiCl. Although some noticeable differences will be observed in the urea aggregation behavior of plaques vs. foams, by and large, it will be demonstrated that the morphological features which are present in foams are comparable to those of plaques with similar recipes. This study will also verify that LiCl affects the phase separation characteristics of actual PU foams in a manner similar to that observed for plaques of similar composition.

In order to understand the interaction of LiCl with various components of the polyether based polyurethane-ureas at the molecular level, quantum mechanical calculations using a DFT approach were performed. Interaction geometries, vibrational spectra, and stability energies of the complexes were determined. The theoretical results obtained fully supported experimental observations.

6.3 Experimental

6.3.1 Materials

Table 6.1 summarizes the recipes utilized for the preparation of the plaques and foams with varied LiCl contents, prepared at Dow Chemical in Freeport, TX. A simple nomenclature scheme is used to identify the different samples. The first letter in the nomenclature scheme is either 'P' or 'F' – indicating a plaque or a foam sample respectively. The next set of digits indicates the water content. For example, 'F4.5' indicates a 4.5 water parts per hundred polyol (pphp) containing foam. This is followed by LC (which stands for lithium chloride) and a number which describes the amount of LiCl added to the formulation. For example, 'LC0.5' would indicate that the formulation contains 0.5 LiCl pphp.

The plaques were based on formulations typically utilized in the preparation of slabstock foams except that a surfactant was not utilized. The soft phase comprised of VORANOL® 3137, which is a 13% EO heterofed polyol with a molecular weight of 3000 g/mol, and an average functionality of 2.79. All formulations were based on 80:20 2,4/2,6-toluene diisocyanate (TDI), maintained at an index value of 100. Water was added at 4.5 pphp, which corresponds to a HS content of 37.0 wt%. LiCl (99+% pure) was procured from Aldrich. The catalyst package, used at a level of 0.2 pphp, was a 5:1 mixture (by weight) of DABCO 33LV® catalyst and DABCO®

BL11 catalyst. Chemical details of the catalysts can be found elsewhere [3]. The procedure used to prepare the plaques has been discussed elsewhere [10,11].

Sample	Water (pphp)	LiCl (pphp)	Rise Time (sec)	Blow-off
P4.5-LC0.0	4.5	0.0	-	-
P4.5-LC0.1	4.5	0.1	-	-
P4.5-LC0.5	4.5	0.5	-	-
P4.5-LC1.0	4.5	1.0	-	-
F4.5-LC0.0	4.5	0.0	66	Good
F4.5-LC0.1	4.5	0.1	73	Medium
F4.5-LC0.5	4.5	0.5	88	No
F4.5-LC1.0	4.5	1.0	90	No

Table 6.1 Sample designations and the Rise Time and Nature of Blow-Off for the Foams

A series of corresponding foams was also made. The same polyol, i.e., VORANOL 3137 was used. The TDI index was maintained at 110. The formulations made use of a catalyst package comprising of 0.2 pphp DABCO 8264 catalyst and 0.3 pphp DABCO T-9 catalyst. The surfactant was TEGOSTAB BF2370 at a level of 1.0 pphp. Chemical details of the catalysts and surfactant can be found elsewhere [3]. The foams prepared were based on 4.5 water pphp so they possessed a HS content identical to that of the plaques (37.0 wt%).

The foams were prepared in a lab scale box-foaming operation utilizing wooden boxes with cross-sectional areas of 15 x 15 square inches. Approximately 800 g of polyol, and the appropriate amounts of aqueous LiCl, catalysts, and surfactant were mixed for 15 seconds at 1800 rpm. This was followed by addition of TDI and stirring at 2400 rpm for 3 seconds. The foaming mixture was then poured into the wooden box. During the foam preparation it was observed that the foams incorporating LiCl did not exhibit a visual blow-off (discussed in detail later). This led to a considerable number of closed cells in the foams containing LiCl, and resulted in shrinkage of the foams as they cooled. To overcome foam shrinkage, foam pads measuring 15 x 15 x 4 cubic inches were cut out from the center of the foam bun and subsequently crushed between metal rollers, thereby mechanically opening the cell windows. The crushing step was carried out approximately 1 h after the foams were prepared. The spacing between the rollers was set at 4” and was decreased in 0.5” intervals to a final spacing of 2”. Each foam pad was crushed four times at each roller spacing.

6.3.2 Methods

The cellular structure of the foams was investigated using a Leo 1550 field-emission scanning electron microscope (FE-SEM). Foam samples of ca. 5 mm thickness were cut from the foam buns and mounted to aluminum stubs using copper tape. The samples were then coated with a ca. 15 nm gold layer using a sputter coater. The microscope was operated at 5 kV and images were taken at magnifications of ca. 30x.

To investigate local ordering (*micro* connectivity) of the HS at the 1-10 Å level, wide-angle x-ray scattering (WAXS) was employed. Small angle x-ray scattering (SAXS) was utilized to study the microphase-separated morphology of the plaque and foams investigated. The procedures for these experiments have been used routinely and are described elsewhere [10,11].

Fourier transform infrared (FTIR) spectroscopy was utilized to evaluate the hydrogen bonding characteristics. A Nicolet 510 spectrometer with a Spectra-Tech ATR attachment employing a horizontal ZnSe crystal was used. The collected spectra were analyzed using Omnic 3.0 software. The scans were normalized using the CH_2 absorbance, which occurs at 2970 cm^{-1}.

TEM was used to compare the urea aggregation behavior in the foams vs. the plaques and also to study the influence of LiCl. Small samples were cut from the plaque or the foam and trimmed using a razor blade in order to expose an area small enough to enable microtomy. A diamond knife was used to cryogenically microtome the trimmed surfaces into ultra-thin sections (ca. 80 nm) on a Reichert-Jung ultramicrotome Ultracut E equipped with a model FC-4D cryo-attachment operating at –90°C. No staining procedure was carried out – the contrast observed in the TEM images is solely a function of differences in electron densities of the different phases. The microtomed sections were collected on 600 mesh copper grids using ethanol. Micrographs were taken using a Philips 420T scanning transmission electron microscope (STEM) operating at an accelerating voltage of 100 kV.

Dynamic mechanical analysis (DMA) was carried out in the tensile mode using a Seiko model 210, as described in earlier studies [10,11]. For the foams, storage moduli were arbitrarily normalized to 3×10^9 Pa in the glassy state to remove the effect of differences in cellular structure and bulk foam densities.

Quantum mechanical calculations were performed using Gaussian98, revision A.6 [19]. Density-functional-theory (DFT) formalism with the three-parameter hybrid-functional of Becke was employed [20]. The DFT is a computationally cost-effective method which includes electron

correlations. It determines the electronic structure of a molecule or a molecular complex by optimizing the electron density instead of the wave function [21], and is known to provide accurate molecular geometries and thermodynamical properties. The basis set chosen was 6-31G(d,p). Zero-point energy corrections did not change the results significantly, so they were neglected in the present treatment. Similarly, the corrections to the basis set superposition errors were not included in the calculations. Model compounds chosen were diethyl ether (DEE), 1,3-dimethylurea (DMU), and a urethane – 1,3-dimethylcarbamate (URET). Structures of the most stable complexes formed between LiCl and these model compounds were calculated using full optimization of all geometrical parameters. Computation of the interaction energy between various donor-acceptor pairs was carried out through a super-molecule approach where the ground state energy of the complex ($E_{COMPLEX}$) is calculated and compared to the sum of the ground state energies (E_1+E_2) of individual components. The interaction energy for the complex, referred to as the stability of the complex, is then defined as $\Delta E_{STABILITY} = (E_1+E_2) - E_{COMPLEX}$.

Molar volumes of model compounds were determined by using a Group Contribution Method (GCM) [22,23]. Volumes of Li^+ and Cl^- ions were also calculated using their ionic radii.

6.4 Results and Discussion

It needs to be mentioned that the foams differ from their plaque counterparts in two major ways. Firstly, the foams incorporate a surfactant for stabilization of the cellular structure whereas plaque formulations do not contain a surfactant. Secondly, the plaques possess a thermal history, which is different from that of the foams. While the plaques used in this study were compressed at 100°C for 1 hour in a hot press; the foams, once formed, were allowed to cool at ambient conditions. However, it will become apparent that the trends observed in the structure-property relationships of plaques are reproduced in foam counterparts – thus making it reasonable to study the effect of different additives on foam morphology using plaques of comparable formulations.

TEM has been widely used to examine the large scale precipitation of the urea phase into ‘urea aggregates’, which possess a greater electron density as compared to the polyol phase and appear as darker regions on the micrographs [3,7,10,11,18]. On inspecting slabstock PU foams, Armistead et al reported these urea aggregates to be ca. 300 nm in size [7]. The size of the urea aggregates is, however, a strong function of the foam recipe since these aggregates have been shown to be smaller in size (ca. 100 nm) in a different slabstock system [18], and also found to

be absent in certain molded foams [3]. Also, the absence or presence of a surfactant in a foam recipe has been shown to influence the degree of urea aggregation [18], as discussed earlier.

A relatively low magnification TEM image of sample P4.5-LC0.0 is presented in Fig 6.1. Recall that P4.5-LC0.0 is a plaque and *does not* incorporate any surfactant. This material exhibits

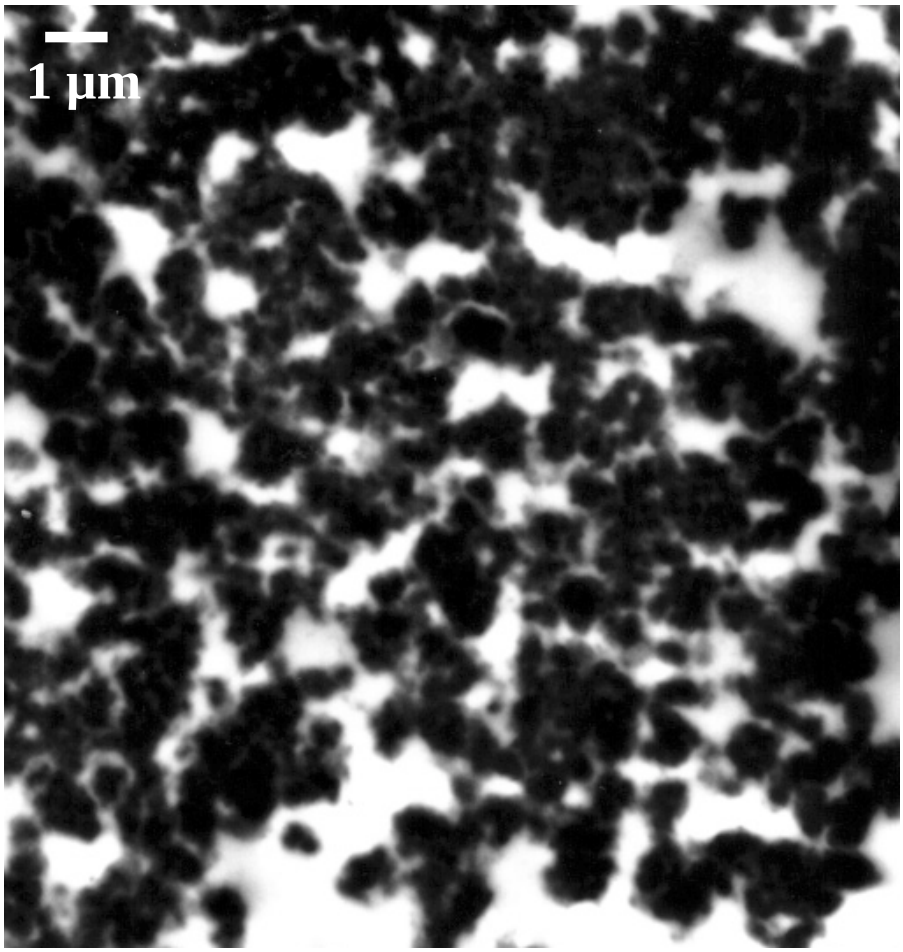

Figure 6.1 Low magnification TEM image of P4.5-LC0.0.

distinct and well-defined urea aggregates which are ca. 1 µm in size. In the same figure equally sized polyol rich regions are also observed. The sample inspected was very stable under the electron beam and there were no signs of beam induced artifacts. In fact, in other studies, samples cut from the same plaque were inspected using AFM [11] and x-ray microscopy [9] and revealed an equivalent morphology as compared to that noted here, confirming that there indeed was no beam damage by TEM.

Microphase separation in polyurethane [24,25] & poly (urethane urea) [26] elastomers, and in PU foam systems [3,4,6,7,10,11,16] has been recurrently investigated using SAXS. In the present study, SAXS was utilized to study the impact of LiCl addition on the urea aggregation and to study microphase separation characteristics. SAXS results for the plaque and foam samples containing the two extremes of LiCl contents investigated, i.e. 0.0 and 1.0 LiCl pphp are

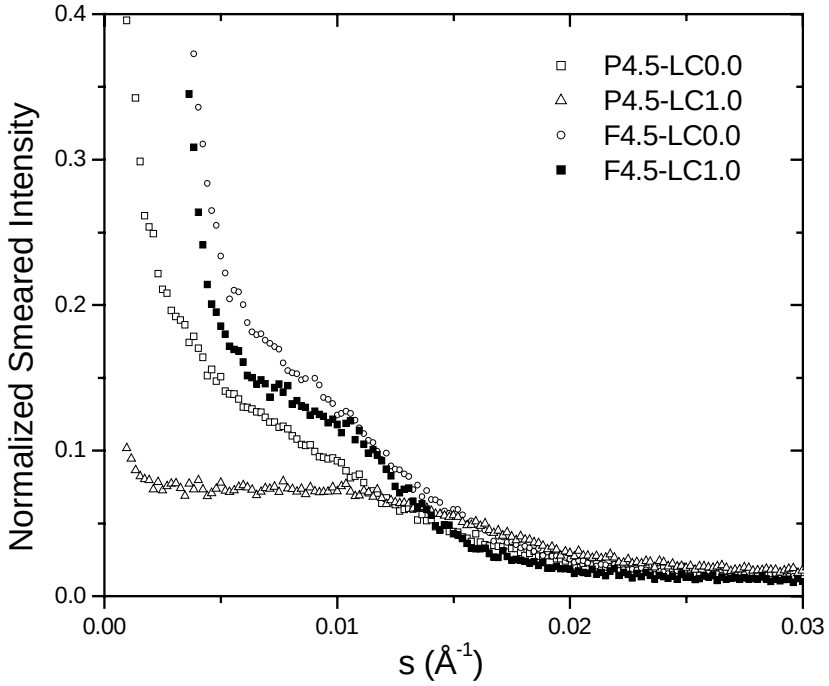

Figure 6.2 Comparison of slit-smeared SAXS profiles of plaques and foams containing the two extremes of LiCl contents (0.0 and 1.0 pphp). A first order interference peak is observed at ca. 100 Å for the plaques and foams with and without LiCl.

displayed in Fig 6.2, where normalized slit-smeared scattered intensity is plotted as a function of the scattering vector 's'. The scattering vector is defined as $s = (2/\lambda)\sin(\theta/2)$ where λ is the wavelength and θ is the radial scattering angle. The presence of a first order interference which appears as a shoulder in all the samples at ca. 0.01 Å^{-1} indicates that all plaques are microphase separated with an average interdomain spacing of ca. 100 Å, in conformity with previously reported results for foam [3,4,6,7] as well as plaque [10,11] formulations.

As noted from Fig 6.2, the SAXS profile of P4.5-LC0.0 exhibits an upturn in the very small angle region where as this behavior is not observed for P4.5-LC1.0. This suggests that the large scale urea aggregates may be contributing to the observed upturn at low 's' values in P4.5-LC0.0. On the other hand, P4.5-LC1.0 displays a substantially lower intensity at low 's' values suggesting that the formation of the urea aggregates is reduced in this formulation. This

observation was also supported by TEM results (presented later) and by noting that the plaque without LiCl was opaque where as P4.5-LC1.0 was relatively transparent. It is also observed that the shoulder associated with P4.5-LC1.0 is much 'sharper' as compared to that of P4.5-LC0.0 implying that a more periodic distribution of the urea microdomains occurs on addition of this additive. In a separate study, on investigating molded PU foam formulations, the author showed that there was a very systematic sharpening of the SAXS shoulder on increasing LiCl content [10]. On comparing the SAXS profiles for the foams, it is seen that both F4.5-LC0.0 and F-4.5-LC1.0 exhibit an upturn in intensity at low 's' values. This upturn is believed to be due to the cellular structure, which is present in both foams. However, on close inspection of the SAXS shoulder region, an effect similar to the one noted for the plaques is observed here – F4.5-LC1.0 exhibits a shoulder, which is relatively sharper as compared to F4.5-LC0.0. This is a strong indication that the *addition of LiCl alters the solid-state microphase separated morphology, (at least at the scale length examined by SAXS) of the foams in a manner similar to that for the plaques*. These results imply that on addition of LiCl, the urea microdomains become more uniformly distributed in the polyol phase.

Figure 6.3 presents high magnification TEM images of the samples for which the SAXS profiles were presented in Fig 6.2. As seen from these images, P4.5-LC0.0 exhibits urea aggregates, which are ca. 500-700 nm in size. This sample, however, exhibited even larger aggregates (~ 1 μm) as seen earlier in Fig 6.1. As hypothesized earlier using SAXS, it is now confirmed in Fig 6.3b that P4.5-LC1.0 shows no signs of urea aggregation, leading to a loss in the *macro* level connectivity of the urea phase. In earlier reports for both slabstock and molded foam based plaques, we showed using SAXS, TEM, and AFM that the urea aggregation systematically decreased as the LiCl content was increased [10,11]. Inspecting the TEM image of F4.5-LC0.0 in Fig 6.3c shows urea aggregates, which are 50-100 nm in dimensions. Comparison of this sample with its plaque counterpart suggests that presence of the surfactant has a significant role in altering the aggregation of the urea phase. Clearly, the presence of the surfactant has influenced the compatibility of the different components in F4.5-LC0.0 as marked by a reduced size of the urea aggregates and also by a weaker contrast between the aggregates and the polyol phase. It should also be recalled that the plaques are compression molded at 100 °C for 1 h, where as the foams do not undergo any such treatment and are allowed to cool at ambient conditions. Subjecting the plaque to these high temperatures and pressures may also be

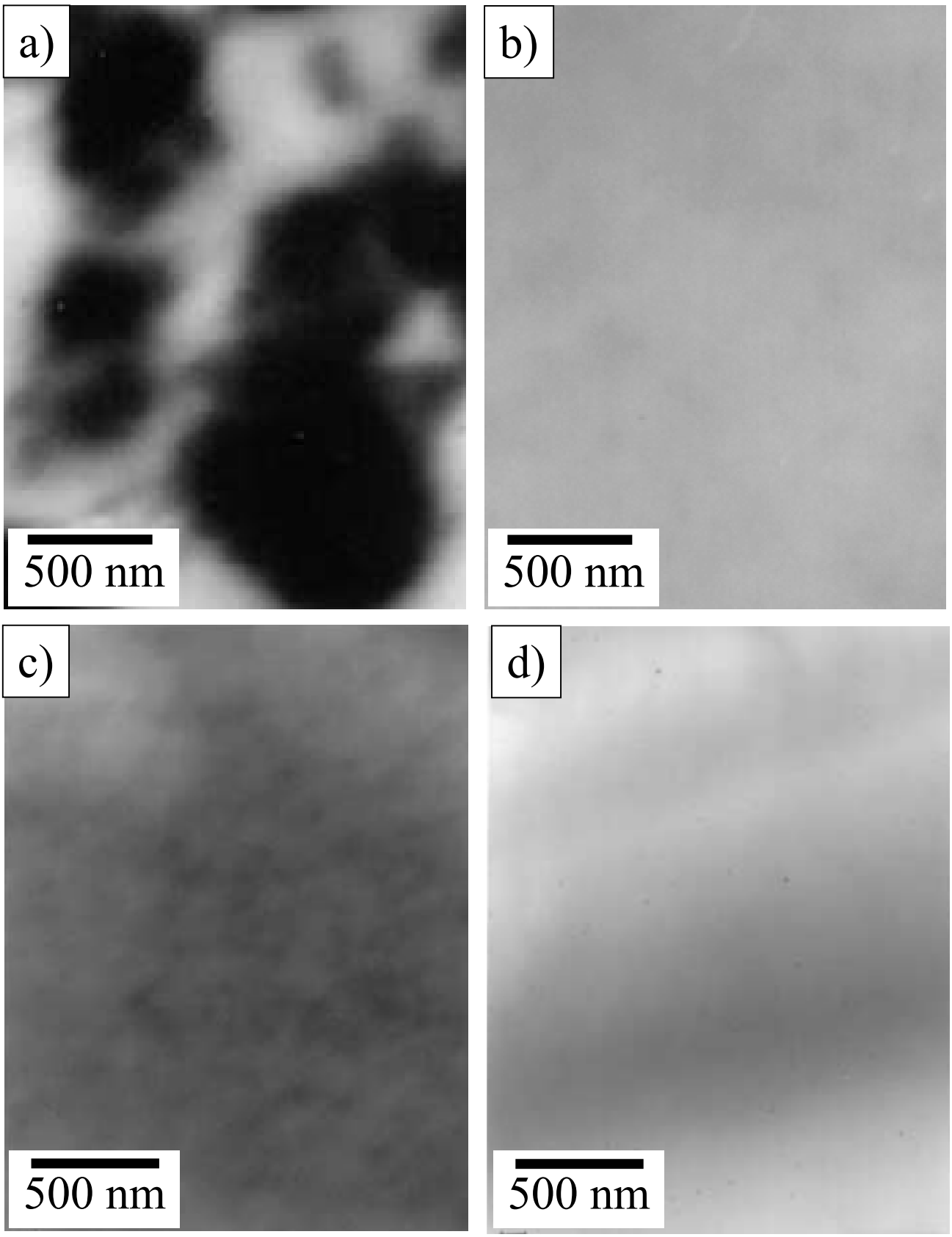

Figure 6.3 Transmission electron micrographs of plaques and foams with and without LiCl a) P4.5-LC0.0, b) P4.5-LC1.0, c) F4.5-LC0.0, and d) F4.5-LC1.0.

influencing the degree of aggregation of the urea phase. Fig 6.3d reveals that there are no signs of urea aggregation in F4.5-LC1.5. *While dissimilarities were noted with regards to the urea aggregation in foams vs. plaques, the influence of LiCl as noted at the scale length via TEM is analogous for both.*

SEM was utilized to examine the cellular structure of foams with and without LiCl. Since LiCl is known to partially block the catalyst which enhances the blow reaction [27], expansion of the LiCl containing foams was observed to be relatively slow during the foaming process. Table 6.1 shows that the "rise time", which is the time required for the foam to reach its final height, systematically increases with LiCl content. From Table 6.1 it is also seen that the foam without LiCl, F4.5-LC0.0, exhibited a good "blow-off" where as this was not true for the foams containing the additive. A "good" blow-off indicates that the CO_2 released in the blow reaction was able escape the foam bun, thus suggesting that some degree of cell-opening was achieved in the foam. The foams incorporating LiCl did not exhibit a good blow-off, and to prevent excessive shrinkage of these foams, they were mechanically crushed between rollers, as outlined earlier. For consistency, the foam which exhibited a good 'blow-off', F4.5-LC0.0, was also crushed in a similar manner. From the above discussion it would be expected that foams with and without LiCl would possess different cellular structures. Fig 6.4 presents SEM images for foams F4.5-LC0.0 and F4.5-LC1.0, parallel and perpendicular to the blow direction. For both materials, the foam cells appear more spherical when viewed parallel to the blow direction (Figs 6.4a, 6.4c). On viewing the same foams in an orthogonal direction (Figs 6.4b, 6.4d) the cells appear more elliptical or elongated. This anisotropy in the cellular structure of slabstock foams and its importance with respect to mechanical behavior has been previously documented [12].

Although the two foams reveal similar cellular structures when viewed parallel to the blow direction, they are noticeably different when viewed perpendicular to the blow direction. As noted from Figs 6.4b and 6.44d, the inability of foam F4.5-LC1.0 to expand sufficiently results in this foam possessing a far greater number of closed windows as compared to foam F4.5-LC0.0. These observations are in agreement with the study carried out by Moreland et al., where it was shown that the foam incorporating LiCl possessed a greater number of closed windows as compared to the foam without the additive [16]. Previous studies have shown that the precipitation of the urea phase and the formation of the urea aggregates are directly related to the cell-opening event in flexible PU foams [28,29]. In fact, one of the mechanisms which leads

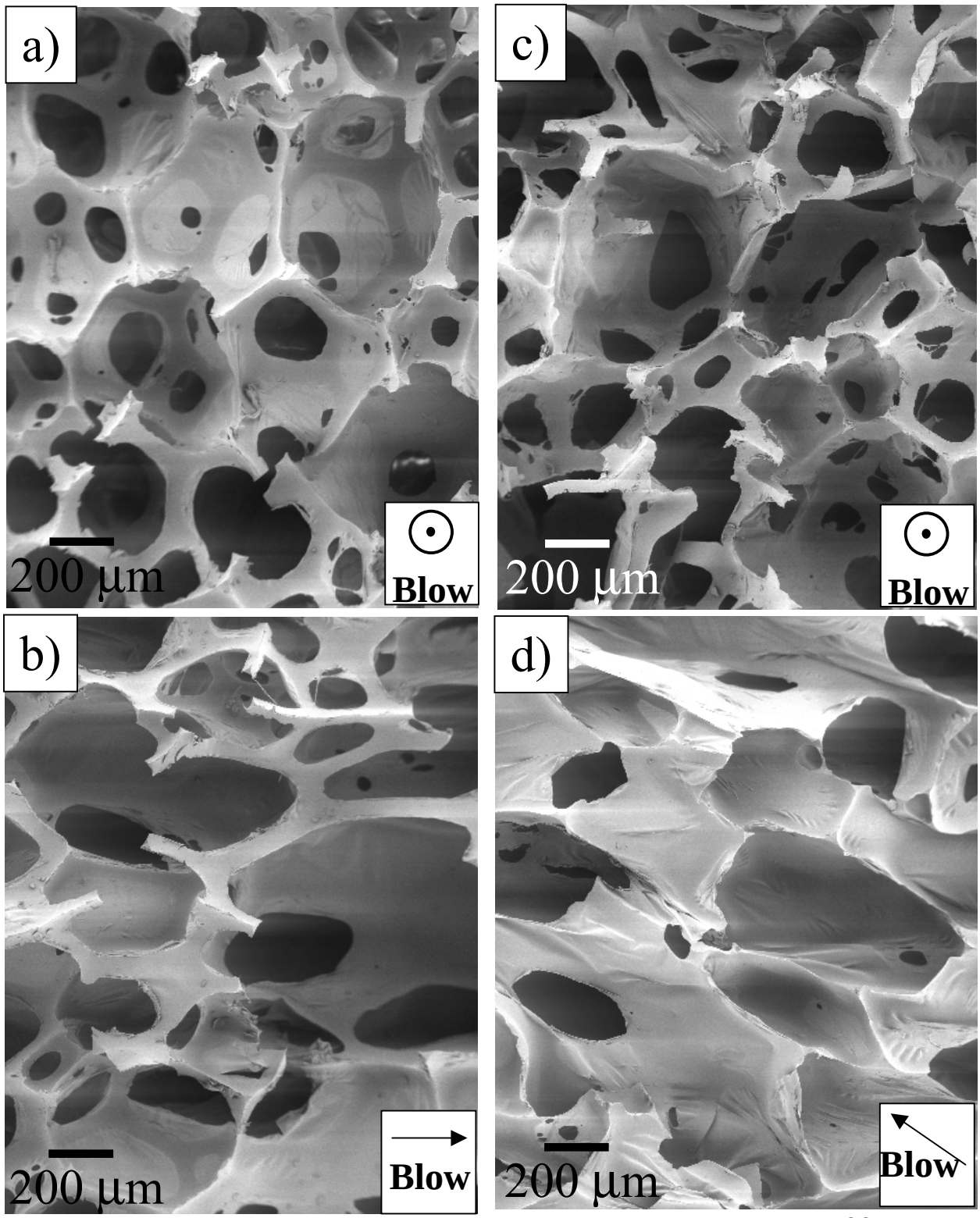

Figure 6.4 Scanning electron micrographs illustrating the cellular structure of foams a) F4.5-LC0.0 viewed parallel to blow direction, b) F4.5-LC0.0 viewed perpendicular to blow direction, c) F4.5-LC1.0 viewed parallel to blow direction, and d) F4.5-LC0.0 viewed perpendicular to blow direction.

to cell-opening is thought to be the formation of urea aggregates where the aggregates act as particulates and lead to cell-opening. Foam F4.5-LC1.0 displays more closed cellular material due to both, the slowing down of the blow reaction which leads to a poor blow-off, as well as due to the lack of formation of urea aggregates in this foam as noted by TEM.

WAXS and FTIR were utilized to examine the regularity in segmental packing of the urea HS within the microdomains. The HS in these materials, due to the asymmetric nature of the

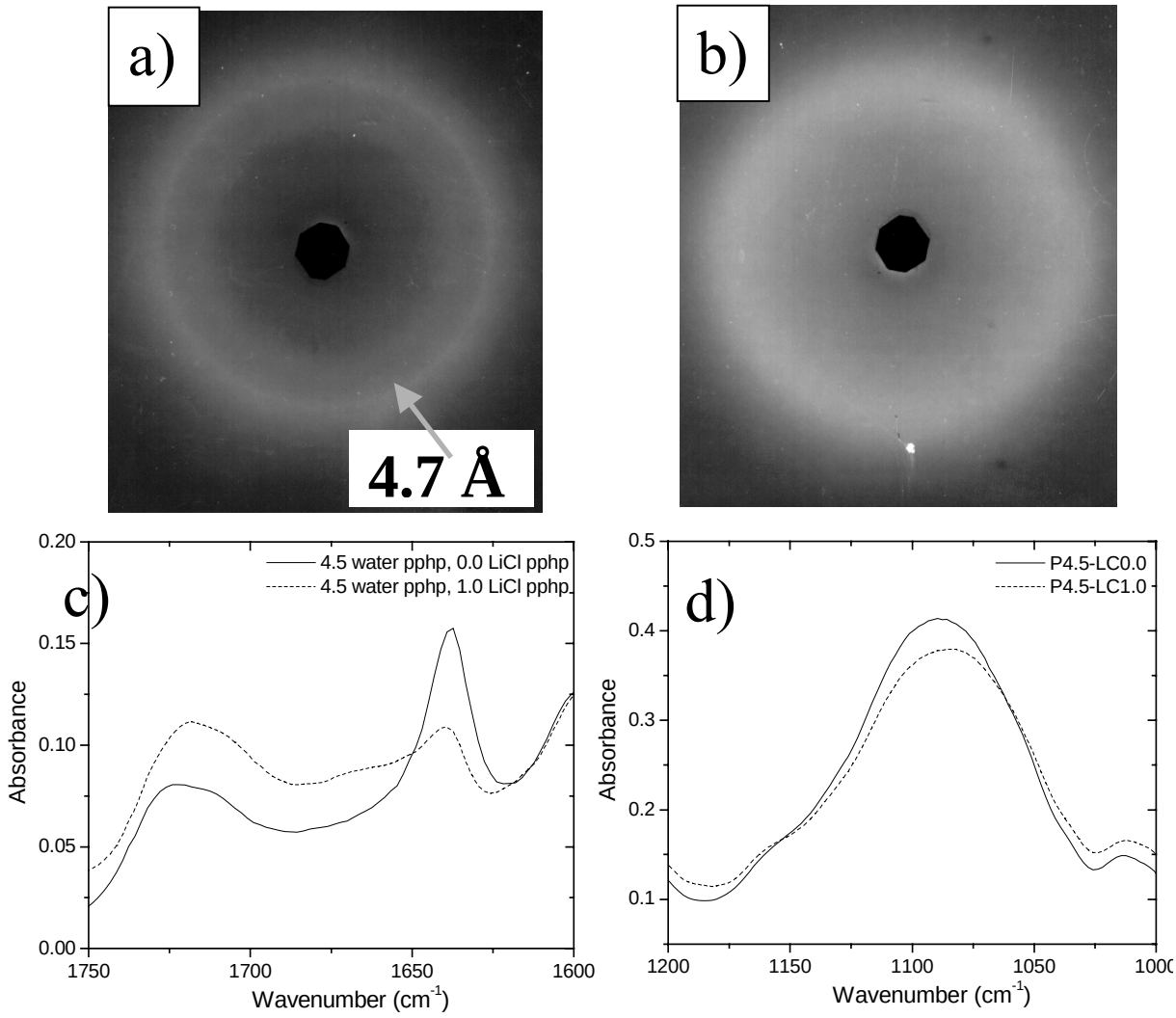

Figure 6.5 a) WAXS pattern for P4.5-LC0.0, b) WAXS pattern for P4.5-LC1.0, c) Portion of FTIR spectrum showing the influence of LiCl on the carbonyl region of the plaques, and d) Portion of FTIR spectrum showing the influence of LiCl on the polyether region of the plaques.

2,4-TDI isomer are not crystalline, but are known to organize via hydrogen bonding in a manner which leads to a 4.7 Å reflection in WAXS [7,18]. The HS packing has also been linked to their strong bidentate hydrogen bonding interactions, associated with a 1640 cm^{-1} absorbance

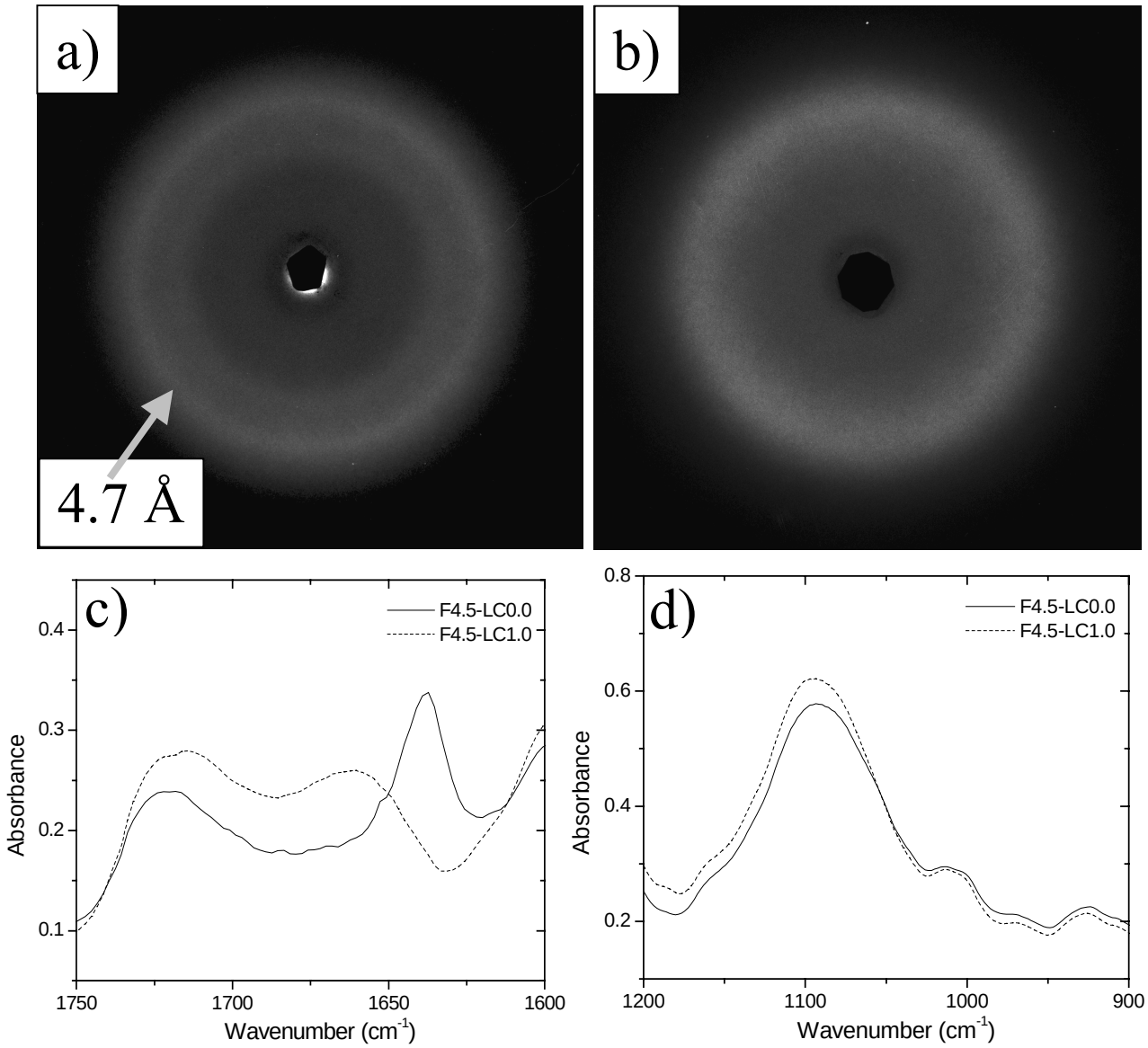

Figure 6.6 a) WAXS pattern for F4.5-LC0.0, b) WAXS pattern for F4.5-LC1.0, c) Portion of FTIR spectrum showing the influence of LiCl on the carbonyl region of the foams, and d) Portion of FTIR spectrum showing the influence of LiCl on the polyether region of the foams.

observed via FTIR [18]. Fig 6.5a displays a distinct 4.7 Å WAXS peak for P4.5-LC0.0 whereas this peak is absent in the 1.0 LiCl pphp plaque (Fig 6.5b). Plaques with intermediate LiCl content show a systematic loss in the peak intensity as LiCl content is increased and are thus not presented. Fig 6.5c shows the FTIR spectra of the carbonyl region for P4.5-LC0.0 and P4.5-LC1.0. The 1640 cm^{-1} absorbance is found to decrease on addition of LiCl, indicative of loss in the bidentate hydrogen bonding, or the *micro* level connectivity of the HS. In the same figure it is noted that, as expected, there is a corresponding increase in the ~ 1715 cm^{-1} absorbance, indicating that the 'free' non-hydrogen bonded urea increases on addition of LiCl. Fig 6.5d displays the FTIR spectra of the CH_2OCH_2 band, which is known to occur at ca. 1060 – 1150 cm^{-1}. In the present case, the position as well as absorption of the peak at ~ 1090 cm^{-1}, which occurs due to the polyether SS, is noted to be similar for plaques with and without LiCl.

The WAXS data for the foams, as presented in Figs 6.6a & 6.6b, are found to be in concert with those for the plaques. Although the 4.7 Å spacing is somewhat weaker in F4.5-LC0.0 as compared to P4.5-LC0.0, it is found to be absent in the foam containing LiCl. The FTIR data for the foams (Fig 6.6c and 6.6d) also shows similar results as exhibited by the plaques. *The observations made in Figs 6.5 and 6.6 further confirm that the influence of LiCl on the morphology of plaques vs. foams is similar, even at the scale length noted by WAXS and FTIR.* In both systems, LiCl clearly restricts the HS from assembling in an ordered form, leading to a loss in the *micro* level connectivity of the urea phase, and causes minimal changes in the soft phase. This observation also indirectly indicates that the LiCl preferentially interacts with the hard phase and hardly influences the soft phase.

DMA is a widely used technique to examine the viscoelastic features of flexible PU foams [3,6,7,11,18]. In Fig 6.7, storage modulus and Tanδ are plotted as a function of temperature for the plaques with varied LiCl contents. All samples display a SS T_g at ca. –50°C, typical of flexible PU foams [3,7]. This is followed by a rubbery plateau region up to ca. 200°C after which degradation begins. Incorporation of LiCl results in altering the DMA behavior in two major ways. Firstly, it is seen from the storage modulus curves that addition of LiCl substantially reduces the temperature range of the rubbery modulus regime, i.e., the LiCl containing plaques lose their cohesiveness at higher temperatures, as indicated by a substantial drop in their storage moduli at ca. 125°C. Secondly, addition of LiCl systematically broadens the SS T_g as observed both in the storage moduli as well as Tanδ graphs. *The trends noted in the*

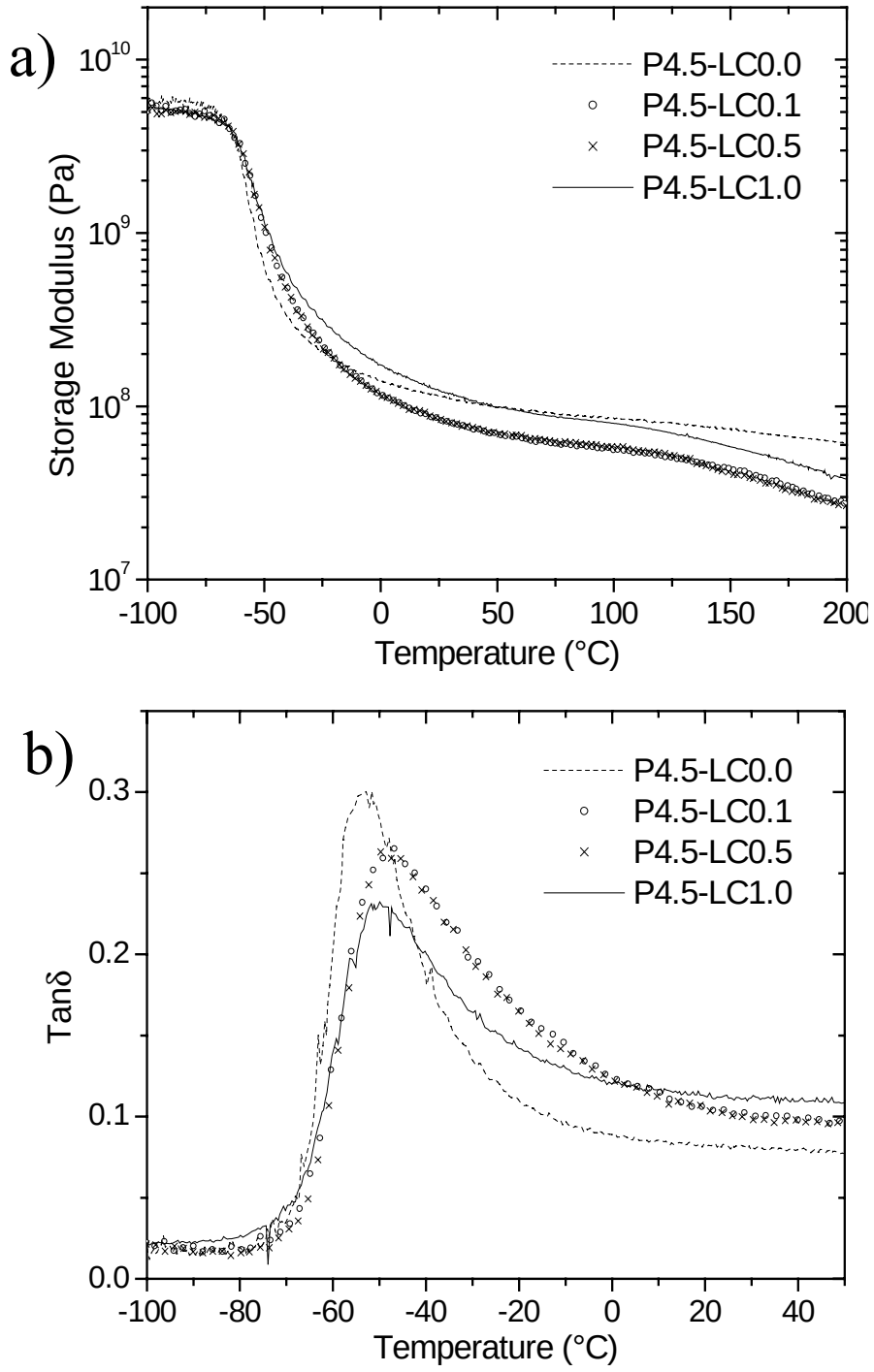

Figure 6.7 Dynamic mechanical analysis results of samples P4.5-LC0.0, P4.5-LC0.1, P4.5-LC0.5, P4.5-LC1.0: a) Storage Modulus, and b) Tanδ.

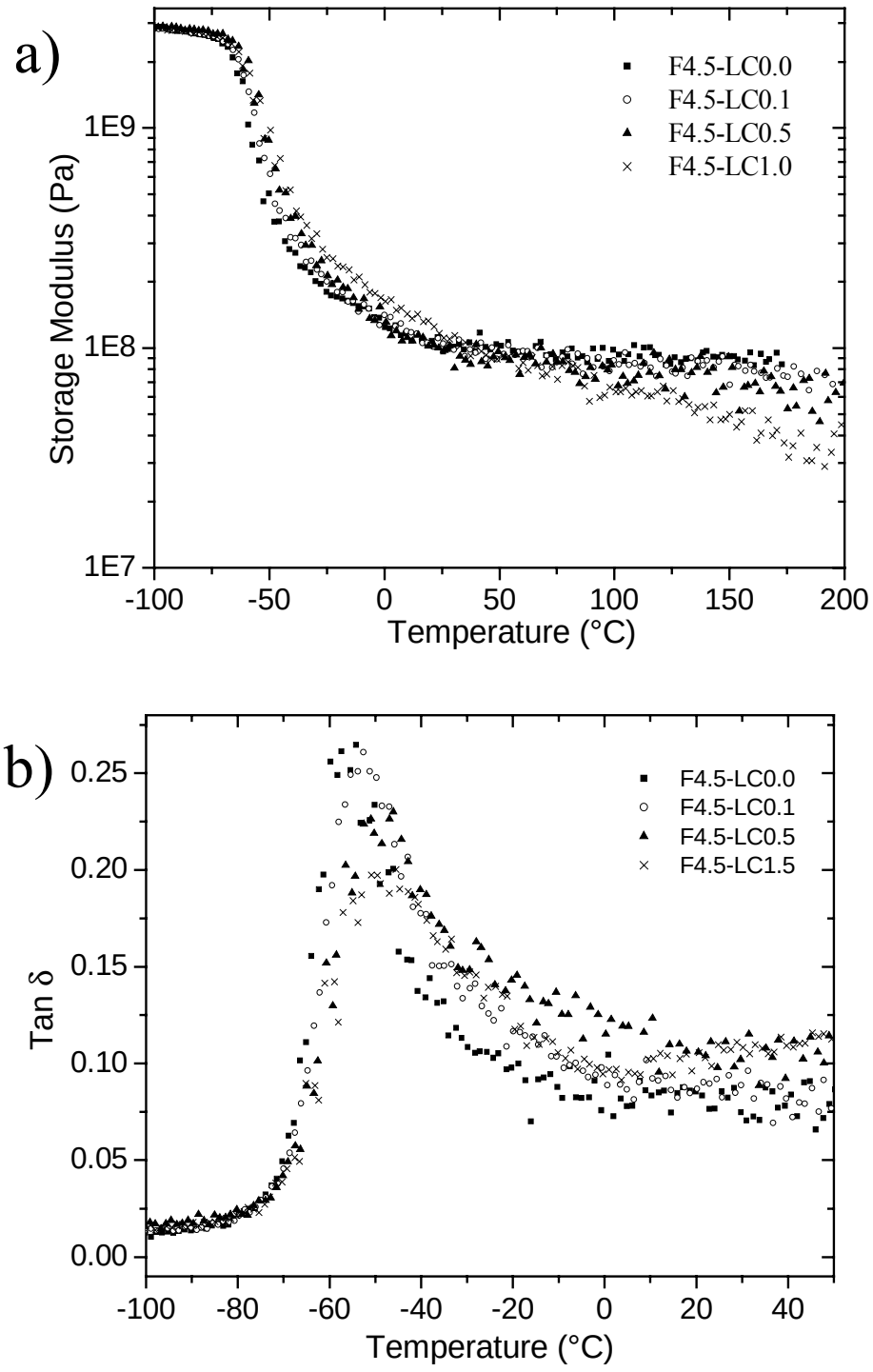

Figure 6.8 Dynamic mechanical analysis results of samples F4.5-LC0.0, F4.5-LC0.1, F4.5-LC0.5, F4.5-LC1.0: a) Storage Modulus, and b) Tanδ.

DMA behavior of the foams, as noted from Fig 6.8, parallel those noted for the plaque counterparts in Fig 6.7. (In order to magnify the SS T_g region, note that the abscissa of the Tanδ graphs in Figures 6.7b and 6.8b have been deliberately plotted with a reduced range of –100 to 50 °C). On close examination of the storage modulus graphs at ca. 25 °C, for both plaques and foams, the rubbery modulus for the 0.1 and 0.5 pphp containing materials is lower than that for the material with no LiCl. However, for the 1.0 LiCl pphp samples, the storage modulus is actually greater than that of the sample devoid of LiCl. This somewhat surprising behavior was reported and confirmed using other complimentary techniques in earlier work from our laboratory [11]. It was suggested that at lower LiCl contents (0.1 and 0.5 LiCl pphp) there occurs a loss in the urea phase *macro* connectivity and also of the filler-like effect caused by the urea aggregates leading to the lowering of the modulus. As the LiCl content is increased, the urea microdomains become more homogeneously distributed (as observed by SAXS and TEM) and impose mobility restrictions on the SS fraction (as observed by DMA). This leads to the 1.0 LiCl pphp systems possessing a modulus greater than that of the materials which do not contain LiCl.

The present study also strongly suggests that LiCl preferentially interacts with the hard domains as compared to the soft polyol phase. The basis for this hypothesis stems from the SAXS, TEM, WAXS, and carbonyl region of the FTIR data, which show considerable changes in the association of the urea phase on LiCl addition. In addition, the corresponding SS T_g (DMA) and the ether region of FTIR display insignificant changes in the soft phase on addition of LiCl. Also, as the foaming reactions proceed, the urea microdomains and aggregates are expected to form in the water rich regions of the inhomogeneous foaming mixture; and since LiCl has an affinity for water, it would also be anticipated to be present in the hard phase.

In order to understand the interaction of LiCl with various components of the polyurethane-urea foam or plaque materials at the molecular level, quantum mechanical calculations using the DFT approach were also carried out. For a better understanding of the influence of the ionic sizes of Li^+ and Cl^- on the packing of urea HS, molar volumes of these species and those of model compounds were also calculated (Table 6.2). As seen from this table, Li^+ has a relatively small molar volume (0.55 cm^3/mol) compared to Cl^- which has a fairly large (15.0 cm^3/mol) molar volume. It is clear that, in terms of disrupting the packing order of the urea HS, Cl^- is expected to play a more important role than will Li^+.

	Molar volume (cm^3/mol)	
Model compound or ion	GCM	Ionic radius
Diethyl ether	80.7	–
1,3-Dimethylcarbamate	77.9	–
1,3-Dimethylurea	70.4	–
Li^+	–	0.55
Cl^-	19.5	15.0

Table 6.2 Molar volumes of the model compounds, diethyl ether (DEE), 1,3-dimethylcarbamate (URET), and 1,3-dimethylurea (DMU) as calculated by using the Group Contribution Method (GCM) and molar volumes of the ionic species, Li^+, Cl^- as calculated using their ionic radii.

System	Stabilization energy (kJ/mol)	O ····· Li^+ (Å)	H ····· Cl^- (Å)
DEE–Li^+	–201.1		–
URET–Li^+	–238.5		–
DMU–Li^+	–271.9		–
DEE–Cl^-	12.4	–	
URET–Cl^-	–378.1	–	
DMU–Cl^-	–415.1	–	
DEE–LiCl	–188.7	1.88	
URET–LiCl	–616.6	1.76	1.84
DMU–LiCl	–687.0	1.66	2.08
DMU–LiCl–DEE	–213.0	1.86 (C=O····· Li^+)	
		1.98 (–O– ···· Li^+)	

Table 6.3 Results from quantum mechanical calculations on the interaction of Li^+, Cl^-, and LiCl with model compounds, 1,3-dimethylurea (DMU), 1,3-dimethlycarbamate (URET), and diethyl ether (DEE). Bond lengths and stabilization energies of the complexes formed.

The geometries and stability energies for the complexes formed between Li^+, Cl^- and LiCl with URET, DMU and DEE were determined. Figures 6.9a – 6.9c give the geometries of the most stable complexes formed between LiCl–URET, LiCl–DMU, and LiCl–DEE respectively. As expected, Li^+ interacts with the ether and carbonyl oxygen fairly strongly. On the other hand the Cl^- counterion can only be stabilized by the (N–H) protons of the urethane (Fig 6.9a and Table 6.2) or the urea groups (Fig 6.9b and Table 6.2). Therefore, the Cl^- ion remains at some distance form the DEE backbone (Fig 6.9c) since such an interaction provides little stabilization from an energy point of view. This behavior dramatically influences the stability of the complexes formed. Stabilization energies of all of the complexes investigated are given in Table 6.3, together with the ($O\cdots Li^+$) and ($H\cdots Cl^-$) distances. As given in this table, the stabilization energies of the complexes formed between Li^+ and DEE, URET, and DMU (without any Cl^-) are –201, –239 and –272 kJ/mol respectively. The substantial influence of the Cl^- ion on the stabilization of the complexes formed can easily be seen from the energies of DEE–LiCl, URET–LiCl, and DMU–LiCl systems, which are –189, –617, and –687 kJ/mol respectively. When compared with Li^+ containing systems, the presence of Cl^- reduces the stability of the ether LiCl complex by 12.4 kJ/mol, but, on the other hand, dramatically enhances the stabilities of urethane (–378 kJ/mol) and urea (–415 kJ/mol) complexes, as given in Table 6.3. In order to further investigate the preference of LiCl between DEE and DMU, the geometry of the complex formed between DEE–LiCl–DMU was also determined, as shown in Fig 6.9d. As presented in Table 6.3, the stabilization energy of this complex (–213 kJ/mol) is more negative than that of DEE-LiCl (–189 kJ/mol), but much less negative than that of DMU-LiCl (–687 kJ/mol). In addition to the stabilization energies, calculated $O\cdots Li^+$ distances (Table 6.3) also provide supporting information on the relative strength of interaction between Li^+ and oxygen in DEE, URET, and DMU.

In addition, theoretically determined IR spectrum was obtained for the DEE-Li^+ system. This spectrum showed that if Li^+ were to complex with the ether oxygen, there would be a corresponding shift in the C–O–C stretching absorption from 1125 cm^{-1} for pure DEE, to 1030 cm^{-1} for DEE-Li^+. No such shift arising from the polyether SS was noted in the experimentally determined spectra, as discussed earlier in Figs 6.5 & 6.6, indicating that there indeed is minimal, if any, interaction of Li^+ with the polyol. All of these results obtained by quantum mechanical

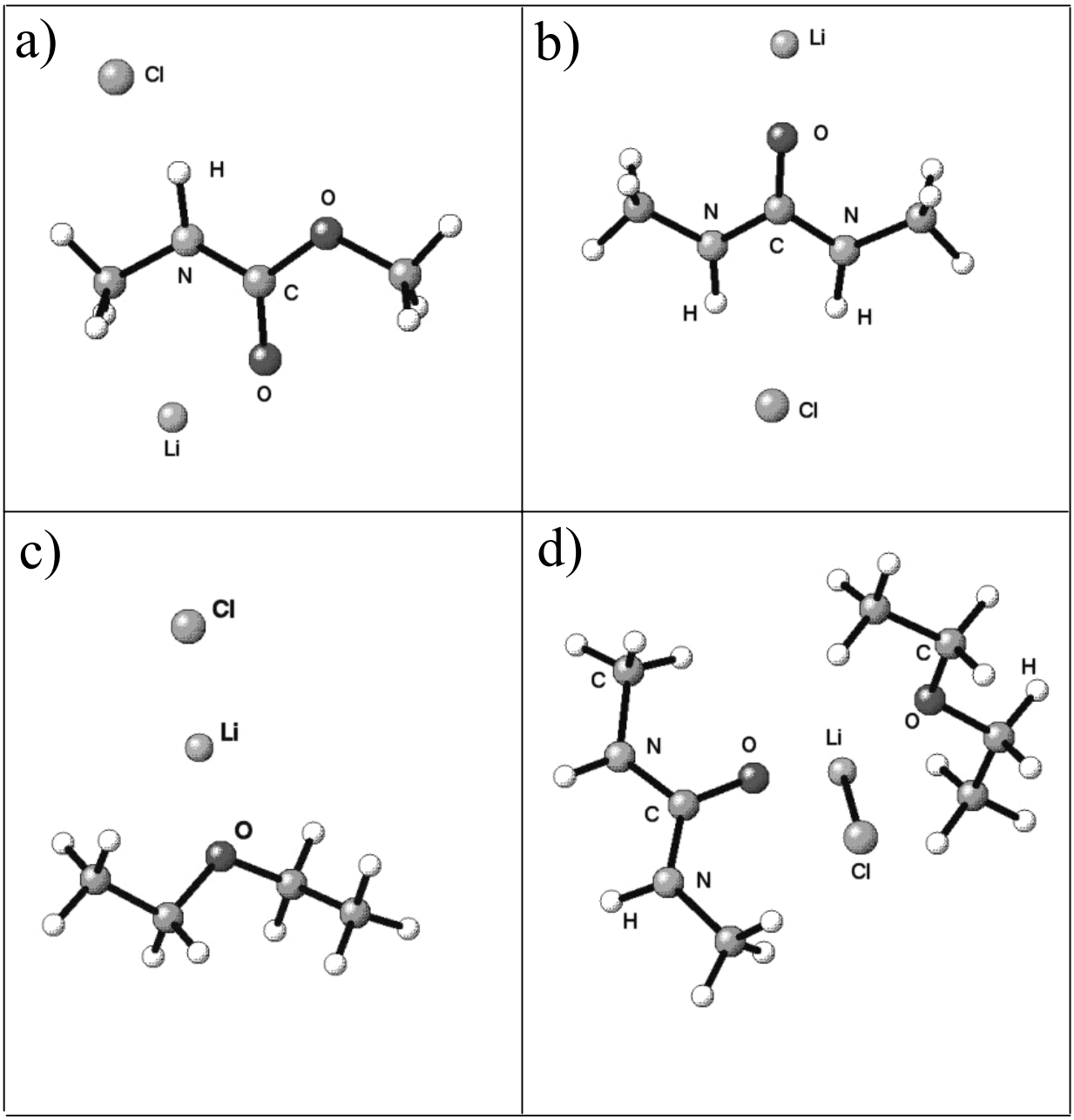

Figure 6.9 Theoretically predicted molecular geometries from DFT calculations a) URET – LiCl Complex b) DMU – LiCl complex c) DEE–LiCl complex d) DMU-LiCl-DEE complex.

calculations clearly indicate that LiCl will preferentially interact with the urea or urethane groups in the foam (or plaque), and not with the polyether. This strongly supports the experimental observations made in the analyses of these systems, particularly using WAXS, FTIR, and DMA. These results also show the power of combining quantum mechanical calculations with experimental data to better understand the local interactions at the molecular level.

6.5 Conclusions

Lithium chloride was used to systematically alter the phase separation characteristics of slabstock flexible PU foams and their plaque counterparts. The resulting morphologies of the foams and plaques were studied at different scale lengths using several characterization techniques. SAXS and WAXS demonstrated that the phase separated morphologies of the plaques and foams are quite comparable when examined at these scale lengths. However, the presence of a surfactant in the foam formulations was shown to considerably reduce the urea aggregation as compared to a plaque with a similar recipe (TEM).

The influence of LiCl on the solid-state microphase separated morphology of both plaques and foams is also demonstrated to be similar. In both systems, LiCl leads to a reduction in urea aggregation (SAXS, TEM) and also interferes in the packing behavior of the HS (WAXS, FTIR). The DMA behavior of the plaques and foams is explained on the basis of changes in morphology. WAXS, DMA and FTIR suggest that the interaction of LiCl is preferentially with the urea HS and insignificant with the polyol SS. This hypothesis is also reinforced using quantum mechanical calculations. Finally, this study further establishes the rationale for the use of plaques to indirectly investigate the solid-state morphology of PU foams, and of additives such as LiCl to probe urea phase connectivity.

6.6 Reference

1. Woods, G. The ICI Polyurethanes Book, 2nd ed.; ICI Polyurethanes and John Wiley and Sons: 1990.
2. Hepburn C. Polyurethane Elastomers, 2nd ed.: Elsevier Applied Science, 1991.
3. Herrington R, Hock K. Flexible Polyurethane Foams, 2nd ed.: Dow Chemical Co.: Midland, MI, 1998.
4. Wilkes GL, Abouzahr S, Radovich D. J Cell Plast 1983;19:248.
5. Elwell MJ, Ryan AJ, Grünbauer HJM, Van Lieshout HC. Macromolecules 1996,;29: 2960.

6. Kaushiva BD, Wilkes GL. J Appl Polym Sci 2000;77:202.
7. Armistead JP, Wilkes GL, Turner RB. J Appl Polym Sci 1988;35:601.
8. Ade H, Smith AP, Cameron S, Cieslinski R, Mitchell G, Hsiao B, Rightor E. Polymer 1995;36:1843.
9. Rightor EG, Urquhart SG, Hitchcock AP, Ade H, Smith AP, Mitchell GE, Priester RD, Aneja A, Appel G, Wilkes GL, Lidy WE. Macromolecules 2002;35:5873.
10. Aneja A, Wilkes GL. J App Polym Sci 2002;85:2956.
11. Aneja A, Wilkes GL. Polymer 2002;43:5551.
12. Moreland JC, Wilkes GL, Turner RB. J Appl Polym Sci 1994;52:549.
13. Abouzahr S, Wilkes GL, Ophir Z. Polymer 1982;23:1077.
14. Seymour RW, Cooper SL. Adv Urethane Sci 1974;3:66.
15. Aneja A, Wilkes GL. Manuscript in preparation.
16. Moreland JC, Wilkes GL, Turner RB, Rightor EG. J Appl Polym Sci 1994;52:1459.
17. Snow SA, Stevens RE. Silicone Surfactants Edited by Hill RM, Marcell Dekker Inc. 1999, p. 137.
18. Kaushiva BD, McCartney SR, Rossmy GR, Wilkes GL. Polymer 2000;41:285.
19. Gaussian 98, Revision A6, Frisch MJ, Trucks GW, Schlegel HB, Scuseria GE, Robb MA, Cheeseman JR, Zakrzewski VG, Montgomery Jr. JA, Stratmann RE, Burant JC, Dapprich S, Millam JM, Daniels AD, Kudin KN, Strain MC, Farkas O, Tomasi J, Barone V, Cossi M, Cammi R, Mennucci B, Pomelli C, Adamo C, Clifford S, Ochterski J, Petersson GA, Ayala PY, Cui Q, Morokuma K, Malick DK, Rabuck AD, Raghavachari K, Foresman JB, Cioslowski J, Ortiz JV, Stefanov, BB, Liu G, Liashenko A, Piskorz P, Komaromi I, Gomperts R, Martin RL, Fox DJ, Keith T, Al-Laham MA, Peng CY, Nanayakkara A, Gonzalez C, Challacombe M, Gill PMW, Johnson B, Chen W, Wong MW, Andres JL, Gonzalez C, Head-Gordon M, Replogle ES, Pople JA, Gaussian Inc., Pittsburgh PA, 1998.
20. Becke AD. J Chem Phys 1996;104:1040.
21. Kohn W, Becke AD, Parr RG. J Phys Chem 1996;100:12974.
22. Van Krevelen DW, Properties of Polymers, Elsevier, Amsterdam, 1990, Ch. 7.
23. Porter D, Group Interaction Modeling of Polymers, Marcel Dekker, New York, 1995.
24. Neumüller W, Bonart R. J Macromol Sci Phys 1974;B(9)3:447.
25. Koberstein JT, Stein RS. J Polym Sci Polym Phys 1983;21:1439.
26. Garrett JT, Runt J, Lin JS. Macromolecules 2000;33:6353.
27. Priester RD. Dow Chemical Co., personal communication.
28. Rossmy GLW, Schator H, Wiemann M, Kollmeier HJ. J Cell Plast 1981;17:319.
29. Neff RA, Macosko CW. Rheologica Acta 1996;35:656.